

The 2024–2025 Seismic Sequence in the Santorini–Amorgos Region: Insights Into Volcano-Tectonic Activity Through High-Resolution Seismic Monitoring

Ioannis Fountoulakis  * ¹, Christos P. Evangelidis  ¹

¹Institute of Geodynamics, National Observatory of Athens, Greece

Author contributions: *Conceptualization:* Ioannis Fountoulakis, Christos P. Evangelidis. *Methodology:* Ioannis Fountoulakis. *Software:* Ioannis Fountoulakis. *Formal Analysis:* Ioannis Fountoulakis, Christos P. Evangelidis. *Writing - Original draft:* Ioannis Fountoulakis, Christos P. Evangelidis,. *Writing - Review & Editing:* Ioannis Fountoulakis, Christos P. Evangelidis,. *Supervision:* Christos P. Evangelidis.

Abstract The 2024–2025 seismic sequence in the Santorini–Amorgos region demonstrates complex tectonic-volcanic interactions. In this study, a detailed seismic catalog is presented, generated for operational monitoring using machine-learning-based phase picking and high-precision relocation. By late summer 2024, seismic activity emerged beneath Santorini, then appeared at around 20 km beneath Kolumbo before migrating northeastward and shallower around Anydros, aligning with southwest-northeast tectonic structures. The relocation confirmed diffuse migration, with some shallow events. Non-double couple moment tensors and spectral metrics suggest crack-opening driven by magmatic and fluid involvement. These findings point to upward migration of magmatic fluids from deep reservoirs or dike injection.

Non-technical summary Between 2024 and 2025, the Santorini–Amorgos region experienced a complex series of earthquakes linked to both tectonic and volcanic causes. Using advanced tools for accurate detection and location, we established a daily monitoring system to keep authorities informed and to build a detailed earthquake catalog. Over time, the earthquakes shifted from Santorini to nearby areas such as Kolumbo, Anydros, and southwest of Amorgos. By analyzing earthquake waves, we found signs that some events were caused by cracks opening, likely due to magma movement at depth. These findings suggest a dynamic interaction between tectonic forces and volcanic activity. All data products are publicly available for future research.

Production Editor:
Kiran Kumar Thingbaijam
Handling Editor:
Tiegan Hobbs
Copy & Layout Editor:
Tara Nye

Received:
March 24, 2025
Accepted:
May 22, 2025
Published:
May 29, 2025

1 Introduction

At the end of January 2025, intense seismic activity emerged in the broader Santorini–Amorgos (SA) region, causing unrest among residents of nearby islands. However, this was not an isolated phenomenon as several minor seismic events had been observed on Santorini Island over the past six months, as indicated by seismic observations from the Institute for the Study and Monitoring of Santorini Volcano (<https://ismosav.gr>). In early March, activity continued, though with fewer events and lower magnitudes. The affected region lies within one of the most active volcanic centers of the South Aegean Volcanic Arc (SAVA), which has formed by the ongoing subduction of the African plate beneath the Eurasian plate (e.g., Pichon and Angelier, 1979; Papanikolaou, 1993) (Fig. 1a). This subduction process is driven by slab retreat, a key mechanism controlling the geodynamic evolution, which has also influenced the present-day extensional deformation and volcanism of the Aegean (e.g., Jolivet et al., 2013).

The area of interest is located within the broader

SA Fault Zone, which serves as a transitional zone between the western and eastern segments of the Volcanic Arc. This fault zone exhibits a right-lateral transtensional character, with NW–SE-directed extension, and acts as a major structural boundary that subdivides the arc into a relatively quiet western part and a seismically and volcanically active eastern part (Bohnhoff et al., 2006; Tsampouraki-Kraounaki et al., 2021). Inside the SA Fault Zone, multiple basins are observed (Christiana, Anydros, Santorini-Anafi, and Amorgos) that are bounded by major extensional to transtensional faults (e.g., Sakellariou et al., 2017; Preine et al., 2022) (Fig. 1b). The extended Santorini volcanic center, with Santorini (Thera) volcano at its core, also includes the Christiana Islands and the submarine Kolumbo volcano, all aligned along a NE–SW lineament. These sites have been extensively studied over the years (e.g., Sigurdsson et al., 2006; Nomikou et al., 2012, 2013). Both volcanic centers exhibit active volcano-tectonic behavior (e.g., Bohnhoff et al., 2006; Dimitriadis et al., 2009; Andinisari et al., 2021b), with well-studied structures (Heath et al., 2019; Hooft et al., 2019; McVey et al., 2019). The most recent significant volcanic unrest occurred dur-

*Corresponding author: ifountoul@noa.gr

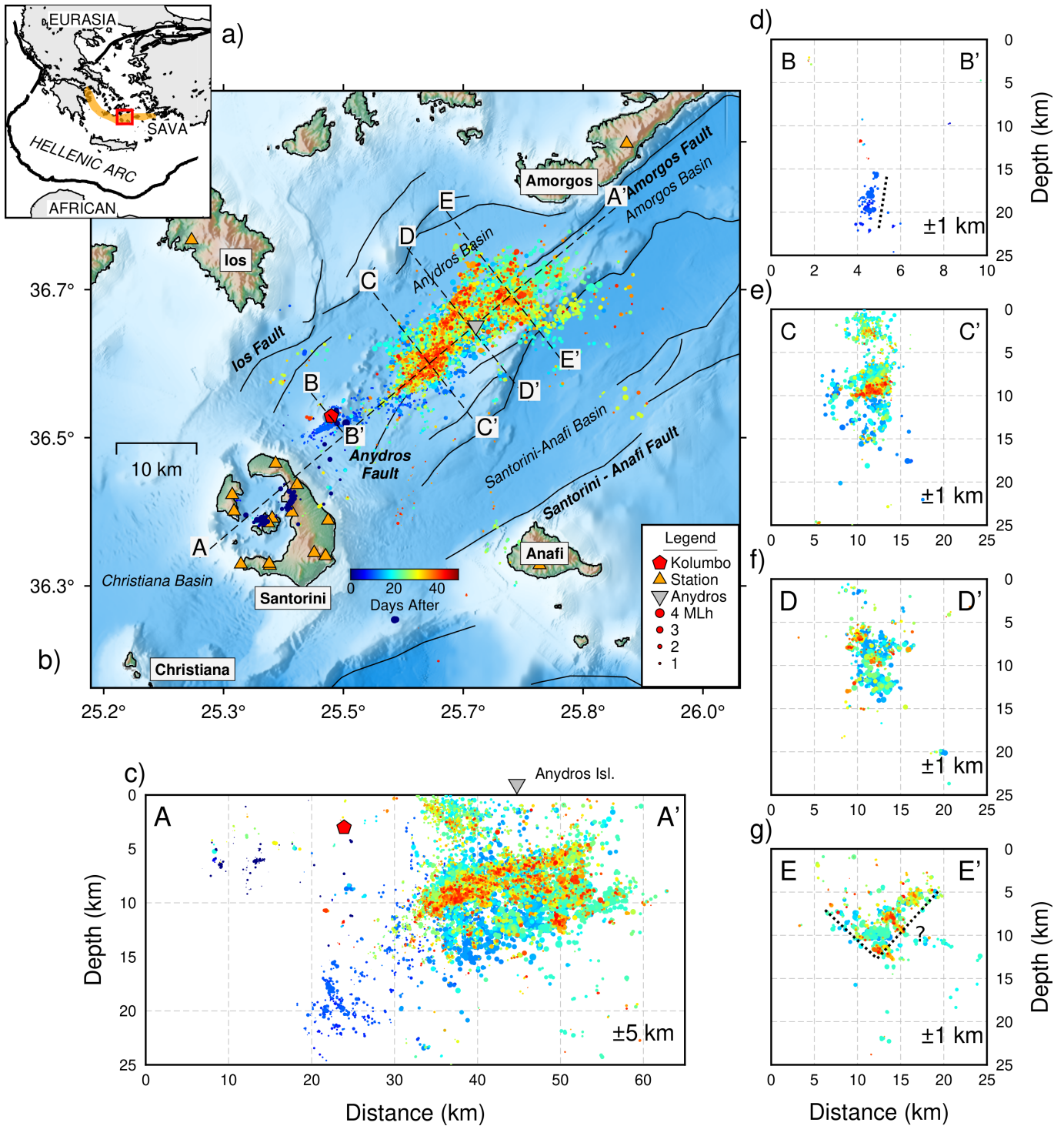


Figure 1 (a) General illustration of the broader Hellenic arc region, showing the main plate boundaries. The South Aegean Volcanic Arc (SAVA) is highlighted in orange, with the study area shown in b) marked by a red rectangle. (b) Relocated seismic events, color-coded based on their occurrence date relative to 20/01/2025 (DD:MM:YYYY) and scaled according to their local magnitude (M_L). Black lines represent the main fault traces in the area (Nomikou et al., 2018), while the red polygon defines the Kolumbo volcano chamber (2–4 km depth based on Chrapkiewicz et al. (2022)). The inverted triangle marks the location of Anydros Island, and triangles indicate the seismic stations used in this study. Vertical cross-sections (c)–(g) are also shown, with the dashed lines in (d) and (g) to denote inferred activated structures.

ing 2011–2012 in Santorini, marked by microseismicity within the caldera and crustal deformation linked to magmatic body intrusion without an eruption (e.g., Newman et al., 2012; Saltogianni et al., 2014; Papadimitriou et al., 2015).

Based on previous work on other seismic sequences in Greece (Fountoulakis et al., 2023; Evangelidis and

Fountoulakis, 2023), we investigated the seismological characteristics of the ongoing activity in the SA region using automated workflows to enhance the National Observatory of Athens (NOA) seismic catalog and refine structural imaging. To construct the updated seismic catalog, we employed a deep-learning phase picker (Mousavi et al., 2020), a rapid association method

(Münchmeyer, 2024), absolute location and relocation techniques (Lomax et al., 2014; Lomax and Savvaidis, 2021), and a relative relocation approach (Trugman and Shearer, 2017). Additionally, we determined as many moment tensor (MT) solutions as possible using Gisola (Triantafyllis et al., 2021), and we analyzed the type of events using automatic frequency content analysis.

2 Data and methods

2.1 Building a new catalog

Based on the seismicity rates, the period from 01/06/2024 to 06/03/2025 (DD:MM:YYYY format used throughout the text) was selected to study the seismic sequence (Fig. S1), as it captures the onset and peak of the activity. Continuous waveforms were used from 22 broadband and short-period seismometers and 1 strong-motion station within 150 km from the area under unrest (Fig. 1, S1a). More details about the data availability can be found in Text S1. For the identification of P- and S-wave seismic phases, the EQTransformer signal detector by Mousavi et al. (2020) was deployed, integrated into the Seisbench package (Woollam et al., 2022). EQTransformer is a deep-learning picker based on an attention mechanism which allows the model to focus on relevant features in the waveform data. It is designed to detect seismic signals in continuous waveforms and identify primary and secondary arrivals. It has been widely used for seismic event detection in various circumstances (e.g., Scotto di Uccio et al., 2022; Fountoulakis et al., 2023; Drooff and Freymueller, 2023; Peña Castro et al., 2024). We adopted the model trained on the VCSEIS benchmark dataset (Zhong and Tan, 2024), which incorporates seismic waveforms from various volcanic regions worldwide, as it quickly became evident that volcanic activity might be involved based on characteristic features observed in the spectrograms and supported by moment tensor analysis. Zhong and Tan (2024) demonstrated that the performance of existing deep-learning-based phase pickers tends to decline in environments with lower-frequency earthquake signals, such as volcanic regions. However, their proposed model showed improved performance, making it particularly well-suited to our specific monitoring context.

The independently identified phases were associated and initially located using PyOcto (Münchmeyer, 2024), a 4-D space–time node partitioning algorithm that identifies and validates, through a grid search approach, the space–time node from which a set of picks most likely originates. A 1-D velocity model (Fig. S2), compiled from various local studies (Papazachos and Nolet, 1997; Dimitriadis et al., 2010; Heath et al., 2019), was employed within PyOcto and used throughout this study. After associating phases, the newly identified events were more accurately located using NonLinLoc (Lomax et al., 2000, 2014). Events with low quality (azimuthal gaps $> 300^\circ$, average rms > 0.5 s, and horizontal-vertical error > 5 km) were removed. Subsequently, seismic events were relocated using the source-specific station

term (SSST) correction method (Richards-Dinger and Shearer, 2000; Lin and Shearer, 2005), which can significantly enhance the absolute location accuracy of the events by reducing the travel-time residuals. We applied the NonLinLoc implementation of the SSST method, which follows an approach similar to the shrinking-box SSST technique (Lin and Shearer, 2005). In our case, the process started with a 40 km smoothing width and underwent five iterations, halving the box size. Keeping the same quality criteria as in the previous step, the final SSST catalog consisted of 20473 well-located seismic events based on the events errors (Fig. S3). The earthquake locations were further refined using the GrowClust approach (Trugman and Shearer, 2017), which employs hierarchical clustering and relocates events based on waveform similarity through a cross-correlation (CC) approach. Waveforms were cross-correlated for event pairs recorded at common stations using a band-pass filter between 2 and 10 Hz, after being tested for an adequate signal-to-noise ratio (≥ 5). More details about the CC results are given in Figure S4. To achieve high relocation precision, only event pairs with minimum CC values of at least 0.7 (e.g., Schaff and Waldhauser, 2005; Trugman et al., 2020; Lin et al., 2022) in minimum six phases were considered. Out of the 20,473 events in the input catalog, 13,952 events were successfully relocated ($\sim 68\%$). Relative relocation uncertainties were estimated through bootstrapping with 50 resamplings of the input CC data, yielding median horizontal and vertical errors of approximately 0.7 km and 0.5 km, respectively (Fig. S5). We used a multi-step event location workflow, with each step designed to progressively enhance location accuracy. Finally, the local magnitudes of the catalog were estimated using the local magnitude (M_L) scale of Scordilis et al. (2015) with a magnitude of completeness (M_c) of the dataset ranging from 1.5 to 1.7 (Fig. S6). The GrowClust catalog is regarded as the final catalog and will be used for further analysis in the next sections.

2.2 Moment tensors

The MT is a vital tool to quantify and describe the type of the seismic source. In the current study, MTs were calculated using an updated version of the Gisola software (Triantafyllis et al., 2021). Gisola is a high-performance application of the classic ISOLA approach (Sokos and Zahradnik, 2013; Zahradník and Sokos, 2018), a method based on waveform inversion for computing centroid moment tensors using single- or multiple-point-source models. Gisola also includes additionally a 4-D spatiotemporally adjustable grid for the centroid determination. The updated version of Gisola used in this study includes the capability for full MT inversion, which was not available in the original package. Seismic events from the final relocated catalog with $M_L \geq 3.5$ were analyzed using the software, and a subset was selected after careful inspection. Initially, solutions grouped as C or D based on the categorization of Scognamiglio et al. (2009) were discarded. Subsequently, the variance reduction (VR), the condition number (CN), the focal-mechanism variability index (FMVAR) and the space–time variabil-

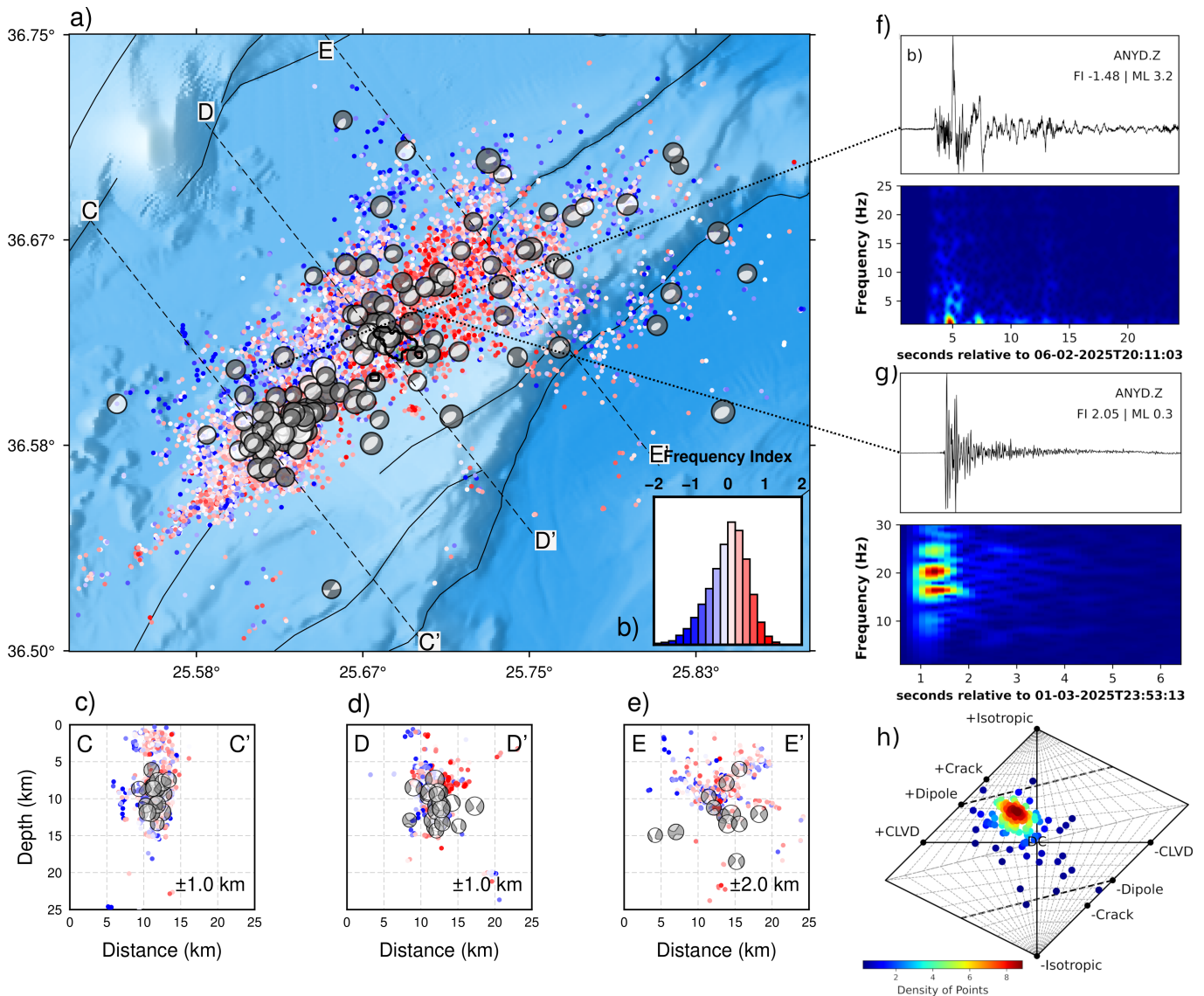


Figure 2 (a) Map view of seismicity distribution, colored by Frequency Index (FI) values, with calculated focal mechanisms shown as black beach balls. The black outline represents Anydros Island. (b) Distribution of FI values. (c)–(e) Vertical cross-sections, similar to Figure 1. (f) and (g) Waveform examples along with their spectrograms. (h) Hudson source-type plot (Hudson et al., 1989).

ity index (STVAR) were examined based on the uncertainty assessment framework of Sokos and Zahradnik (2013), where these parameters are explained in detail. For a solution to be considered successful in this study, we adopt the following uncertainty thresholds: $VR \geq 0.5$, $CN \leq 5$, $FMVAR \leq 30^\circ$, and $STVAR \leq 0.40$. A solution is discarded if it fails to meet at least two of the previously mentioned parameters. From the aforementioned process we managed to compute 133 high-quality and stable MT solutions (Fig. 2, S7) with the uncertainty results presented in Figure S8.

2.3 Type of seismic signals

One of the key challenges in this study is the identification of seismic signal types, which is essential for understanding of the source processes. To better characterize potential complexity of these events, we adopted an automated approach to analyze the frequency content of earthquakes as a quantitative metric. For the

relocated earthquake catalog, the Frequency Index (FI) spectral ratio metric (Buurman and West, 2010) is estimated. This method, which calculates the mean amplitude within a low and high frequency spectral band, quantifies the spectral content of individual events (e.g., Ketner and Power, 2013; Matoza et al., 2014). However, instead of the mean amplitude, we used the integrated power spectral amplitude similar to Anderson et al. (2025). Although FI is often used to classify events presumed to be volcanic, in this study it is applied solely to explore the frequency content distribution of the signals. This allows us to identify patterns that may suggest different underlying source processes, without assigning events to fixed categories. A high (positive) FI signifies the prevalence of high-frequency energy characteristic of brittle failure, tectonic earthquakes, or volcano-tectonic earthquakes (Lahr et al., 1994), while a low (strongly negative) FI denotes the predominance of low-frequency energy, frequently linked to fluid-driven mechanisms such as the resonance of fluid-filled frac-

tures or conduits triggered by pressure transients in the fluid (Aki et al., 1977; Chouet, 1988). The FI was calculated for each event using an 8 s time window following the theoretical P-wave arrival at the ANYD station, which was the closest station to the events origin, to minimize path effects that could distort the frequency content. Events were included in the analysis if they were recorded from ANYD and if the signal-to-noise ratio exceeded 5 in both frequency bands. The results of the MTs and FI analysis can be found in Figure 2.

3 Results and discussion

Our relocated catalog increases significantly the number of detected events, providing a more detailed visualization of the activated systems. As already analyzed, seismic activity began months ago within the Santorini caldera (Fig. 1b, S9), forming two main clusters, one at the center of the caldera and another in the northeastern part of the island (Fig. 1b). Both have persisted with low-level seismicity as indicated by the seismicity rates and with depths between 2 and 9 km (Fig. 1c, S9). A similar seismicity pattern was also observed during the 2011–2012 unrest period (Konstantinou et al., 2013). After January 25, 2025, as seismicity rates on Santorini remained stable, seismic activity began to appear northeast of the island beneath the Kolumbo volcano at depths between 17 and 22 km. The seismicity formed a linear, vertical, narrow pattern beneath Kolumbo (Fig. 1d) and persisted for approximately 5–6 days, with relatively small-magnitude events (< 1.0 – 1.5). It then gradually migrated northeast, close to Anydros islet, and at shallower depths (Fig. 1c). Here, at depths between 10 and 15 km, the seismicity formed a dominant plateau, creating a stable seismogenic layer where seismic activity persisted for the remainder of the study period, affecting a disrupted area approximately 20 km in length with a diffuse character extending about 10 km in width. (Fig. 1 and 2). A vertical cross-section, subparallel to the extended SW–NE tectonic structures, clearly shows that the seismicity follows a trajectory from deeper within the crust beneath Kolumbo and gradually shallowing towards the northeast (Fig. 1c). The northeasternmost disrupted area, near Amorgos, is forming smaller linear branches and is located close to the southwestern edge of the Amorgos fault that has been activated during the 1956 M_w 7.6 earthquake (e.g., Okal et al., 2009; Leclerc et al., 2024). Some cross-sections (Fig. 1e,f) suggest relative vertical-dipping structures, though the seismicity appears to be diffuse. The cross-section at the northeasternmost part of the area shows antithetic structures (Fig. 1g). Additionally, earthquakes seem to cluster near other significant geological structures, running parallel to the main activity (near Amorgos Fault). Notably, there is a significant number of shallow clustered events at depths of less than 5 km, particularly southwest of Anydros, as shown in the cross-sections (Fig. 1c,e).

Figure 3 displays the spatiotemporal behavior of the activity along a SW–NE line between Santorini and Amorgos islands. The spatiotemporal seismicity shows possible back-and-forth migration patterns, with the

most prominent activity occurring between February 11 and February 14. This fast migration had transition velocities that reached up to approximately 2.8 km/h. The MTs observed in the area (Fig. 2) are characterized by positive isotropic (ISO) and compensated linear vector dipole (CLVD) components in most cases (Fig. 2f). Non-double-couple values may be associated with various physical processes, including explosions, volcanic eruptions, or structural collapses. However, their interpretation requires careful consideration and assessment of other seismicity parameters, as non-double-couple values can also reflect inversion artifacts (e.g. Vavryčuk, 2014; Rösler et al., 2024). Positive ISO and CLVD values have been systematically observed in volcanic environments and can be connected to magmatic intrusion (e.g. Dahm and Brandsdottir, 1997; Alvizuri and Tape, 2016). Andinisari et al. (2021a) also reported significant ISO and CLVD signals in the SA area, both positive and negative in Kolumbo, and positive near Anydros, linking them to the opening and closing of cracks caused by the steady migration of magmatic fluids. Moreover, for the studied 2024–2025 activity, Zahradnik et al. (2025) reported only positive ISO and CLVD values, attributing them to a shear-tensile source process (crack opening). However, we also identified instances suggesting a shear-compressional process, such as crack closing (Fig. 2h). The double couple part of the focal solutions is dominated by normal faulting, with NE–SW strike and dip mostly in the 40–60 degrees range, with very few cases of strike-slip nature (Fig. S7). The extensional regime is also confirmed by the calculated stress axes (Fig. S10).

The relative distribution of low- and high-frequency signal components has been mapped with the FI metric. Examining the spatiotemporal distribution of FI values, we observe that medium- to low-FI events are abundant in the area, with high-FI events also present. Higher-FI events are concentrated from Anydros to the northeast, whereas medium- to low-FI events are more prevalent to the southwest and at the northern edge of the NNE–SSW elongate cluster. Most low-FI events occurred before 12-02-2025, after which a decline is observed (Fig. S11a,b). This spatial pattern could imply that the southwest section reflects less tectonic characteristics compared to the northeast. A comparison between FI and double-couple percentage demonstrates that most moment tensors exhibit negative FI values (Fig. S11c) (signals dominated by lower frequencies). Figure S12 and Figure 2f,g presents three distinct cases of waveform data recorded during the crisis, highlighting the complexity of the observed seismic signals. These cases include: (1) a series of numerous high-frequency bursts occurred in the center of the C–C' cross section (Fig. 1), (2) a single low-frequency event, and (3) a high-frequency event.

4 Conclusions

This study presents a seismic analysis of the 2024–2025 activity in the SA region, deploying advanced phase-picking techniques and high-precision relocation methods. The newly created catalog significantly improves

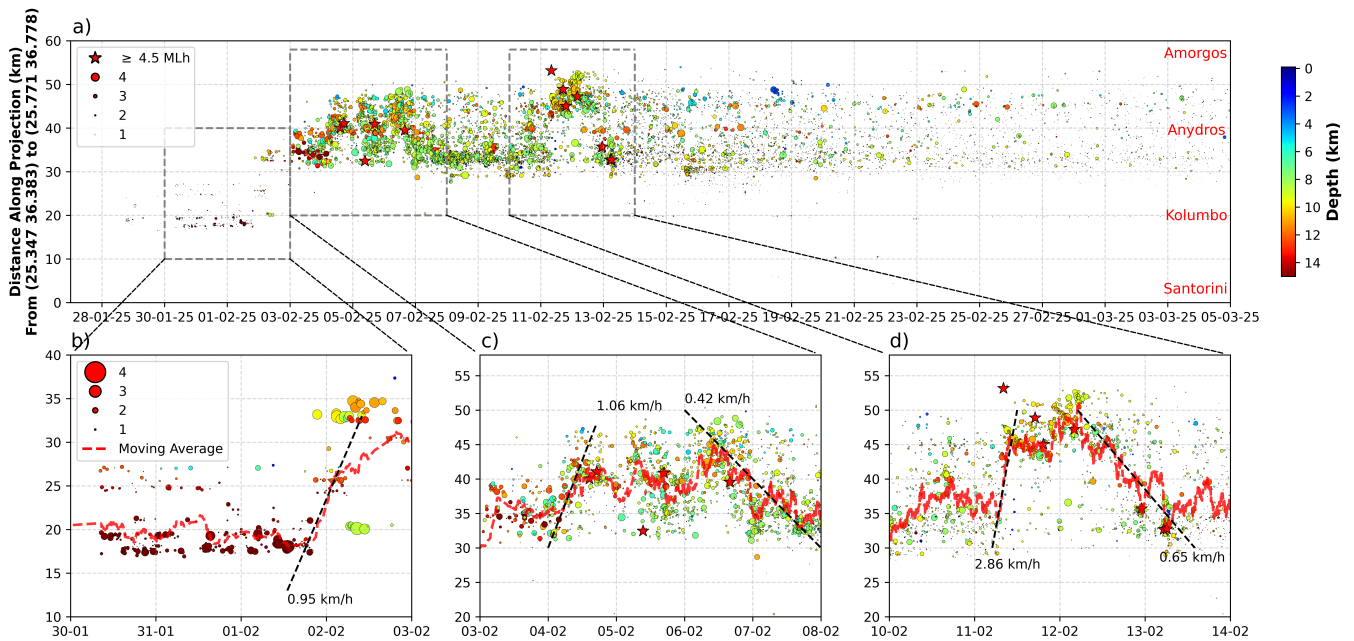


Figure 3 Spatiotemporal projection of epicenters after January 27, 2025 along a straight SW–NE line connecting Santorini and Amorgos island. The width of the projection window was chosen to include all the seismicity along the SW–NE profile. Epicenters are color-coded based on depth and scaled according to their local magnitude (M_L). All $M_L > 4.5$ events are marked with a star and colored red for emphasis. (a) Overview of seismic activity, with panels (b), (c), and (d) showing zoomed-in views of selected time periods with significant unrest and superimposed moving averages. Dashed line slopes indicate areas with possible migration patterns.

event detection and spatial resolution, revealing distinct seismic clusters and migration patterns. By late summer 2024, seismic activity appeared beneath Santorini and within the caldera, but by late January 2025 it moved northeast toward Kolumbo, Anydros and southwest of Amorgos. There, the seismicity initiated at depth (~ 20 km) beneath the Kolumbo volcano and then migrated northeast and to shallower depths, aligning along southwest–northeast-trending tectonic structures. The relocation process confirmed a diffused back and forth migration along this direction with some distinct shallower events SW of Anydros. MT solutions indicate a dominant normal-faulting regime, consistent with regional tectonics, but the presence of positive ISO and CLVD components suggests the involvement of magmatic and fluid processes. The spectral analysis of seismic signals with the FI metric further supports this interpretation, highlighting variations in frequency content that may correspond to different source mechanisms. The observed evidence suggests a complex interplay between tectonic and magmatic processes, making possible an upward migration of magmatic fluids from deep reservoirs or even dike injection. More detailed conclusions can be drawn from the integration of seismic, geodetic, and petrological studies, which could provide deeper insights into the underlying processes of the activity. Nevertheless, this study delivers a higher-quality seismic catalog, generated through an established workflow that was initially developed for daily operational monitoring of the ongoing activity. This catalog is now openly available for future studies.

Acknowledgements

Figures and maps were created using the Pythonic interface of the Generic Mapping Tools (PyGMT) software (Tian et al., 2025) and the Matplotlib library (Hunter, 2007). Additionally, parts of the analysis were conducted using ObsPy (Beyreuther et al., 2010). We are thankful to all those scientists and personnel who maintain and operate their networks at the National Observatory of Athens—Institute of Geodynamics, Aristotle University of Thessaloniki—Seismological Station, and National Kapodistrian University of Athens—Seismological Laboratory. The authors would like to thank C.B. Papazachos from the Aristotle University of Thessaloniki for the valuable discussions and for providing the local velocity model, as well as to P. Nomikou from the National and Kapodistrian University of Athens for supplying local fault data and bathymetric information. Finally, the authors sincerely thank the Editor Tiegan Hobbs, and the reviewer Ryo Okuwaki for their valuable and constructive feedback, which significantly enhanced the quality of this article.

Data and code availability

Seismic records were acquired from the HL (National Observatory of Athens, Institute of Geodynamics, Athens, 1975), HT (Aristotle University of Thessaloniki, 1981), and HA (University of Athens, 2008) networks, accessed through the National Observatory of Athens (NOA) EIDA node (Evangelidis et al., 2021). The following codes are available at the respective links: Gisola (<https://github.com/nikosT/Gisola>) (updated ver-

sion used in this study is currently under development and not yet publicly available), NonLinLoc (<https://github.com/ut-beg-texnet/NonLinLoc>), Growclust (<https://github.com/dttrugman/GrowClust>). All websites were last accessed in March 2025. The supplemental material includes additional figures that provide further details on the study's results. Moreover, the relocated earthquakes, the MTs catalog, and a movie presenting the spatiotemporal evolution of the sequence are openly provided in <https://zenodo.org/records/15074928>.

Competing interests

The authors have no competing interests.

References

- Aki, K., Fehler, M., and Das, S. Source mechanism of volcanic tremor: fluid-driven crack models and their application to the 1963 kilauea eruption. *Journal of Volcanology and Geothermal Research*, 2(3):259–287, Sept. 1977. doi: 10.1016/0377-0273(77)90003-8.
- Alvizuri, C. and Tape, C. Full moment tensors for small events ($M_w \leq 3$) at Uturuncu volcano, Bolivia. *Geophysical Journal International*, 206(3):1761–1783, July 2016. doi: 10.1093/gji/ggw247.
- Anderson, E. C., Parnell-Turner, R., Sohn, R. A., and Fan, W. Deformation on Rainbow massif, Mid-Atlantic Ridge, illuminated with microearthquakes detected by machine learning. *Geophysical Research Letters*, 52(2), Jan. 2025. doi: 10.1029/2024gl111285.
- Andinisari, R., Konstantinou, K., and Ranjan, P. Moment tensor inversion of microearthquakes along the Santorini-Amorgos zone: Tensile faulting and emerging volcanism in an extensional setting. *Journal of Volcanology and Geothermal Research*, 420: 107394, Dec. 2021a. doi: 10.1016/j.jvolgeores.2021.107394.
- Andinisari, R., Konstantinou, K., and Ranjan, P. Seismicity along the Santorini-Amorgos zone and its relationship with active tectonics and fluid distribution. *Physics of the Earth and Planetary Interiors*, 312:106660, Mar. 2021b. doi: 10.1016/j.pepi.2021.106660.
- Aristotle University of Thessaloniki. Aristotle University of Thessaloniki Seismological Network, 1981. doi: 10.7914/SN/HT.
- Beyreuther, M., Barsch, R., Krischer, L., Megies, T., Behr, Y., and Wassermann, J. ObsPy: A Python Toolbox for Seismology. *Seismological Research Letters*, 81(3):530–533, May 2010. doi: 10.1785/gssrl.81.3.530.
- Bohnhoff, M., Rische, M., Meier, T., Becker, D., Stavrakakis, G., and Harjes, H.-P. Microseismic activity in the Hellenic Volcanic Arc, Greece, with emphasis on the seismotectonic setting of the Santorini–Amorgos zone. *Tectonophysics*, 423(1–4):17–33, Sept. 2006. doi: 10.1016/j.tecto.2006.03.024.
- Buurman, H. and West, M. E. *Seismic precursors to volcanic explosions during the 2006 eruption of Augustine Volcano: Chapter 2 in The 2006 eruption of Augustine Volcano, Alaska*. 2010. doi: 10.3133/pp17692.
- Chouet, B. Resonance of a fluid-driven crack: Radiation properties and implications for the source of long-period events and harmonic tremor. *Journal of Geophysical Research: Solid Earth*, 93 (B5):4375–4400, May 1988. doi: 10.1029/jb093ib05p04375.
- Chrapkiewicz, K., Paulatto, M., Heath, B. A., Hooft, E. E. E., Nomikou, P., Papazachos, C. B., Schmid, F., Toomey, D. R., Warner, M. R., and Morgan, J. V. Magma Chamber Detected Beneath an Arc Volcano With Full-Waveform Inversion of Active Source Seismic Data. *Geochemistry, Geophysics, Geosystems*, 23 (11), Nov. 2022. doi: 10.1029/2022gc010475.
- Dahm, T. and Brandsdottir, B. Moment tensors of microearthquakes from the Eyjafjallajökull volcano in South Iceland. *Geophysical Journal International*, 130(1):201–219, July 1997. doi: 10.1111/j.1365-246x.1997.tb00997.x.
- Dimitriadis, I., Karagianni, E., Panagiotopoulos, D., Papazachos, C., Hatzidimitriou, P., Bohnhoff, M., Rische, M., and Meier, T. Seismicity and active tectonics at Coloumbo Reef (Aegean Sea, Greece): Monitoring an active volcano at Santorini Volcanic Center using a temporary seismic network. *Tectonophysics*, 465 (1–4):136–149, Feb. 2009. doi: 10.1016/j.tecto.2008.11.005.
- Dimitriadis, I., Papazachos, C., Panagiotopoulos, D., Hatzidimitriou, P., Bohnhoff, M., Rische, M., and Meier, T. P and S velocity structures of the Santorini–Coloumbo volcanic system (Aegean Sea, Greece) obtained by non-linear inversion of travel times and its tectonic implications. *Journal of Volcanology and Geothermal Research*, 195(1):13–30, Aug. 2010. doi: 10.1016/j.jvolgeores.2010.05.013.
- Drooff, C. and Freymueller, J. T. New Insights Into the Active Tectonics of the Northern Canadian Cordillera From an Enhanced Earthquake Catalog. *Journal of Geophysical Research: Solid Earth*, 128(12), Dec. 2023. doi: 10.1029/2023jb026793.
- Evangelidis, C. and Fountoulakis, I. Imaging the Western Edge of the Aegean Shear Zone: The South Evia 2022–2023 Seismic Sequence. *Seismica*, 2(1), July 2023. doi: 10.26443/seismica.v2i1.1032.
- Evangelidis, C. P., Triantafyllis, N., Samios, M., Boukouras, K., Kontakos, K., Ktenidou, O.-J., Fountoulakis, I., Kalogeras, I., Melis, N. S., Galanis, O., Papazachos, C. B., Hatzidimitriou, P., Scordilis, E., Sokos, E., Paraskevopoulos, P., Serpetsidaki, A., Kaviris, G., Kapetanidis, V., Papadimitriou, P., Voulgaris, N., Kasaras, I., Chatzopoulos, G., Makris, I., Vallianatos, F., Kostantinidou, K., Papaioannou, C., Theodoulidis, N., Margaritis, B., Piliidou, S., Dimitriadis, I., Iosif, P., Manakou, M., Roumelioti, Z., Pitilakis, K., Riga, E., Drakatos, G., Kiratzi, A., and Tselentis, G.-A. Seismic Waveform Data from Greece and Cyprus: Integration, Archival, and Open Access. *Seismological Research Letters*, 92 (3):1672–1684, Mar. 2021. doi: 10.1785/0220200408.
- Fountoulakis, I., Evangelidis, C. P., and Ktenidou, O.-J. Coseismic and Postseismic Imaging of a Composite Fault System: The Samos 2020 M_w 7.0 Sequence. *Bulletin of the Seismological Society of America*, 113(3):997–1012, Mar. 2023. doi: 10.1785/0120220207.
- Heath, B. A., Hooft, E. E. E., Toomey, D. R., Papazachos, C. B., Nomikou, P., Paulatto, M., Morgan, J. V., and Warner, M. R. Tectonism and Its Relation to Magmatism Around Santorini Volcano From Upper Crustal P Wave Velocity. *Journal of Geophysical Research: Solid Earth*, 124(10):10610–10629, Oct. 2019. doi: 10.1029/2019jb017699.
- Hooft, E., Heath, B., Toomey, D., Paulatto, M., Papazachos, C., Nomikou, P., Morgan, J., and Warner, M. Seismic imaging of Santorini: Subsurface constraints on caldera collapse and present-day magma recharge. *Earth and Planetary Science Letters*, 514: 48–61, May 2019. doi: 10.1016/j.epsl.2019.02.033.
- Hudson, J. A., Pearce, R. G., and Rogers, R. M. Source type plot for inversion of the moment tensor. *Journal of Geophysical Research: Solid Earth*, 94(B1):765–774, Jan. 1989. doi: 10.1029/jb094ib01p00765.
- Hunter, J. D. Matplotlib: A 2D Graphics Environment. *Computing in Science & Engineering*, 9(3):90–95, 2007. doi: 10.1109/mcse.2007.55.
- Jolivet, L., Faccenna, C., Huet, B., Labrousse, L., Le Pourhiet, L., Lacombe, O., Lecomte, E., Burov, E., Denèle, Y., Brun, J.-P.,

- Philippon, M., Paul, A., Salaün, G., Karabulut, H., Piromallo, C., Monié, P., Gueydan, F., Okay, A. I., Oberhänsli, R., Pourteau, A., Augier, R., Gadenne, L., and Driussi, O. Aegean tectonics: Strain localisation, slab tearing and trench retreat. *Tectonophysics*, 597–598:1–33, June 2013. doi: 10.1016/j.tecto.2012.06.011.
- Ketner, D. and Power, J. Characterization of seismic events during the 2009 eruption of Redoubt Volcano, Alaska. *Journal of Volcanology and Geothermal Research*, 259:45–62, June 2013. doi: 10.1016/j.jvolgeores.2012.10.007.
- Konstantinou, K., Evangelidis, C., Liang, W.-T., Melis, N., and Kalogeras, I. Seismicity, Vp/Vs and shear wave anisotropy variations during the 2011 unrest at Santorini caldera, southern Aegean. *Journal of Volcanology and Geothermal Research*, 267: 57–67, Nov. 2013. doi: 10.1016/j.jvolgeores.2013.10.001.
- Lahr, J., Chouet, B., Stephens, C., Power, J., and Page, R. Earthquake classification, location, and error analysis in a volcanic environment: implications for the magmatic system of the 1989–1990 eruptions at redoubt volcano, Alaska. *Journal of Volcanology and Geothermal Research*, 62(1–4):137–151, Aug. 1994. doi: 10.1016/0377-0273(94)90031-0.
- Leclerc, F., Palagonia, S., Feuillet, N., Nomikou, P., Lampridou, D., Barrière, P., Dano, A., Ochoa, E., Gracias, N., and Escartin, J. Large seafloor rupture caused by the 1956 Amorgos tsunami-genic earthquake, Greece. *Communications Earth & Environment*, 5(1), Nov. 2024. doi: 10.1038/s43247-024-01839-0.
- Lin, G. and Shearer, P. Tests of relative earthquake location techniques using synthetic data. *Journal of Geophysical Research: Solid Earth*, 110(B4), Apr. 2005. doi: 10.1029/2004jb003380.
- Lin, G., Peng, Z., and Neves, M. Comparisons of in situ Vp/Vs ratios and seismic characteristics between northern and southern California. *Geophysical Journal International*, 229(3):2162–2174, Feb. 2022. doi: 10.1093/gji/ggac038.
- Lomax, A. and Savvaidis, A. High-precision earthquake location using source-specific station terms and inter-event waveform similarity. *Journal of Geophysical Research: Solid Earth*, 127(1), Dec. 2021. doi: 10.1029/2021jb023190.
- Lomax, A., Virieux, J., Volant, P., and Berge-Thierry, C. *Probabilistic Earthquake Location in 3D and Layered Models*, page 101–134. Springer Netherlands, 2000. doi: 10.1007/978-94-015-9536-0_5.
- Lomax, A., Michelini, A., and Curtis, A. *Earthquake Location, Direct, Global-Search Methods*, page 1–33. Springer New York, 2014. doi: 10.1007/978-3-642-27737-5_150-2.
- Matoza, R. S., Shearer, P. M., and Okubo, P. G. High-precision relocation of long-period events beneath the summit region of Kilauea Volcano, Hawai'i, from 1986 to 2009. *Geophysical Research Letters*, 41(10):3413–3421, May 2014. doi: 10.1002/2014gl059819.
- McVey, B., Hooft, E., Heath, B., Toomey, D., Paulatto, M., Morgan, J., Nomikou, P., and Papazachos, C. Magma accumulation beneath Santorini volcano, Greece, from P-wave tomography. *Geology*, 48(3):231–235, Dec. 2019. doi: 10.1130/g47127.1.
- Mousavi, S. M., Ellsworth, W. L., Zhu, W., Chuang, L. Y., and Beroza, G. C. Earthquake transformer—an attentive deep-learning model for simultaneous earthquake detection and phase picking. *Nature Communications*, 11(1), Aug. 2020. doi: 10.1038/s41467-020-17591-w.
- Münchmeyer, J. PyOcto: A high-throughput seismic phase associator. *Seismica*, 3(1), Jan. 2024. doi: 10.26443/seismica.v3i1.1130.
- National Observatory of Athens, Institute of Geodynamics, Athens. National Observatory of Athens Seismic Network, 1975. doi: 10.7914/SN/HL.
- Newman, A. V., Stiros, S., Feng, L., Psimoulis, P., Moschas, F., Saltogianni, V., Jiang, Y., Papazachos, C., Panagiotopoulos, D., Karagianni, E., and Vamvakaris, D. Recent geodetic unrest at Santorini Caldera, Greece. *Geophysical Research Letters*, 39(6), Mar. 2012. doi: 10.1029/2012gl051286.
- Nomikou, P., Carey, S., Papanikolaou, D., Croff Bell, K., Sakellariou, D., Alexandri, M., and Bejelou, K. Submarine volcanoes of the Kolumbo volcanic zone NE of Santorini Caldera, Greece. *Global and Planetary Change*, 90–91:135–151, June 2012. doi: 10.1016/j.gloplacha.2012.01.001.
- Nomikou, P., Papanikolaou, D., Alexandri, M., Sakellariou, D., and Rousakis, G. Submarine volcanoes along the Aegean volcanic arc. *Tectonophysics*, 597–598:123–146, June 2013. doi: 10.1016/j.tecto.2012.10.001.
- Nomikou, P., Hübscher, C., Papanikolaou, D., Farangitakis, G., Ruhnau, M., and Lampridou, D. Expanding extension, subsidence and lateral segmentation within the Santorini - Amorgos basins during Quaternary: Implications for the 1956 Amorgos events, central - south Aegean Sea, Greece. *Tectonophysics*, 722: 138–153, Jan. 2018. doi: 10.1016/j.tecto.2017.10.016.
- Okal, E. A., Synolakis, C. E., Uslu, B., Kalligeris, N., and Voukouvalas, E. The 1956 earthquake and tsunami in Amorgos, Greece. *Geophysical Journal International*, 178(3):1533–1554, Sept. 2009. doi: 10.1111/j.1365-246x.2009.04237.x.
- Papadimitriou, P., Kapetanidis, V., Karakonstantis, A., Kaviris, G., Voulgaris, N., and Makropoulos, K. The Santorini Volcanic Complex: A detailed multi-parameter seismological approach with emphasis on the 2011–2012 unrest period. *Journal of Geodynamics*, 85:32–57, Apr. 2015. doi: 10.1016/j.jog.2014.12.004.
- Papanikolaou, D. Geotectonic evolution of the Aegean. *Bulletin of the Geological Society of Greece*, XXVII:33–48, 1993.
- Papazachos, C. and Nolet, G. P and S deep velocity structure of the Hellenic area obtained by robust nonlinear inversion of travel times. *Journal of Geophysical Research: Solid Earth*, 102(B4): 8349–8367, Apr. 1997. doi: 10.1029/96jb03730.
- Peña Castro, A. F., Schmandt, B., Nakai, J., Aster, R. C., and Chaput, J. (Re)Discovering the Seismicity of Antarctica: A New Seismic Catalog for the Southernmost Continent. *Seismological Research Letters*, 96(1):576–594, July 2024. doi: 10.1785/0220240076.
- Pichon, X. L. and Angelier, J. The hellenic arc and trench system: A key to the neotectonic evolution of the eastern mediterranean area. *Tectonophysics*, 60(1–2):1–42, Nov. 1979. doi: 10.1016/0040-1951(79)90131-8.
- Preine, J., Hübscher, C., Karstens, J., and Nomikou, P. Volcano-Tectonic Evolution of the Christiana-Santorini-Kolumbo Rift Zone. *Tectonics*, 41(11), Nov. 2022. doi: 10.1029/2022tc007524.
- Richards-Dinger, K. B. and Shearer, P. M. Earthquake locations in southern California obtained using source-specific station terms. *Journal of Geophysical Research: Solid Earth*, 105(B5): 10939–10960, May 2000. doi: 10.1029/2000jb900014.
- Rösler, B., Stein, S., Ringler, A., and Vackář, J. Apparent Non-Double-Couple Components as Artifacts of Moment Tensor Inversion. *Seismica*, 3(1), Apr. 2024. doi: 10.26443/seismica.v3i1.1157.
- Sakellariou, D., Sigurdsson, H., Alexandri, M., Carey, S., Rousakis, G., Nomikou, P., Georgiou, P., and Ballas, D. ACTIVE TECTONICS IN THE HELLENIC VOLCANIC ARC: THE KOLUMBO SUBMARINE VOLCANIC ZONE. *Bulletin of the Geological Society of Greece*, 43 (2):1056, Jan. 2017. doi: 10.12681/bgs.11270.
- Saltogianni, V., Stiros, S. C., Newman, A. V., Flanagan, K., and Moschas, F. Time-space modeling of the dynamics of Santorini volcano (Greece) during the 2011–2012 unrest. *Journal of Geophysical Research: Solid Earth*, 119(11):8517–8537, Nov. 2014. doi: 10.1002/2014jb011409.

- Schaff, D. P. and Waldhauser, F. Waveform Cross-Correlation-Based Differential Travel-Time Measurements at the Northern California Seismic Network. *Bulletin of the Seismological Society of America*, 95(6):2446–2461, Dec. 2005. doi: 10.1785/0120040221.
- Scognamiglio, L., Tinti, E., and Michelini, A. Real-Time Determination of Seismic Moment Tensor for the Italian Region. *Bulletin of the Seismological Society of America*, 99(4):2223–2242, July 2009. doi: 10.1785/0120080104.
- Scordilis, E. M., Kementzetzidou, D., and Papazachos, B. C. Local magnitude calibration of the Hellenic Unified Seismic Network. *Journal of Seismology*, 20(1):319–332, Oct. 2015. doi: 10.1007/s10950-015-9529-5.
- Scotto di Uccio, F., Scala, A., Festa, G., Picozzi, M., and Beroza, G. C. Comparing and integrating artificial intelligence and similarity search detection techniques: application to seismic sequences in Southern Italy. *Geophysical Journal International*, 233(2): 861–874, Dec. 2022. doi: 10.1093/gji/ggac487.
- Sigurdsson, H., Carey, S., Alexandri, M., Vougioukalakis, G., Croff, K., Roman, C., Sakellariou, D., Anagnostou, C., Rousakis, G., Ioakim, C., Goguo, A., Ballas, D., Misaridis, T., and Nomikou, P. Marine investigations of Greece’s Santorini Volcanic Field. *Eos, Transactions American Geophysical Union*, 87(34):337–342, Aug. 2006. doi: 10.1029/2006eo340001.
- Sokos, E. and Zahradnik, J. Evaluating Centroid-Moment-Tensor Uncertainty in the New Version of ISOLA Software. *Seismological Research Letters*, 84(4):656–665, July 2013. doi: 10.1785/0220130002.
- Tian, D., Uieda, L., Leong, W. J., Fröhlich, Y., Schlitzer, W., Grund, M., Jones, M., Toney, L., Yao, J., Tong, J.-H., Magen, Y., Materna, K., Belem, A., Newton, T., Anant, A., Ziebarth, M., Quinn, J., and Wessel, P. PyGMT: A Python interface for the Generic Mapping Tools, 2025. doi: 10.5281/ZENODO.14868324.
- Triantafyllis, N., Venetis, I. E., Fountoulakis, I., Pikoulis, E.-V., Sokos, E., and Evangelidis, C. P. Gisola: A High-Performance Computing Application for Real-Time Moment Tensor Inversion. *Seismological Research Letters*, 93(2A):957–966, Dec. 2021. doi: 10.1785/0220210153.
- Trugman, D. T. and Shearer, P. M. GrowClust: A Hierarchical Clustering Algorithm for Relative Earthquake Relocation, with Application to the Spanish Springs and Sheldon, Nevada, Earthquake Sequences. *Seismological Research Letters*, 88(2A):379–391, Feb. 2017. doi: 10.1785/0220160188.
- Trugman, D. T., Ross, Z. E., and Johnson, P. A. Imaging Stress and Faulting Complexity Through Earthquake Waveform Similarity. *Geophysical Research Letters*, 47(1), Jan. 2020. doi: 10.1029/2019gl085888.
- Tsampouraki-Kraounaki, K., Sakellariou, D., Rousakis, G., Morfis, I., Panagiotopoulos, I., Livanos, I., Manta, K., Paraschos, F., and Papatheodorou, G. The Santorini-Amorgos Shear Zone: Evidence for Dextral Transtension in the South Aegean Back-Arc Region, Greece. *Geosciences*, 11(5):216, May 2021. doi: 10.3390/geosciences11050216.
- University of Athens. Hellenic Seismological Network, University of Athens, Seismological Laboratory, 2008. doi: 10.7914/SN/HA.
- Vavryčuk, V. Moment tensor decompositions revisited. *Journal of Seismology*, 19(1):231–252, Oct. 2014. doi: 10.1007/s10950-014-9463-y.
- Woollam, J., Münchmeyer, J., Tilmann, F., Rietbrock, A., Lange, D., Bornstein, T., Diehl, T., Giunchi, C., Haslinger, F., Jozinović, D., Michelini, A., Saul, J., and Soto, H. SeisBench—A Toolbox for Machine Learning in Seismology. *Seismological Research Letters*, 93(3):1695–1709, Mar. 2022. doi: 10.1785/0220210324.
- Zahradnik, J., Sokos, E., Roumelioti, Z., and Turhan, F. Positive isotropic components of the 2025 Santorini-Amorgos earthquakes. Feb. 2025. doi: 10.31223/x5jx5k.
- Zahradník, J. and Sokos, E. *ISOLA Code for Multiple-Point Source Modeling—Review*, page 1–28. Springer International Publishing, 2018. doi: 10.1007/978-3-319-77359-9_1.
- Zhong, Y. and Tan, Y. J. Deep-Learning-Based Phase Picking for Volcano-Tectonic and Long-Period Earthquakes. *Geophysical Research Letters*, 51(12), June 2024. doi: 10.1029/2024gl108438.

The article *The 2024–2025 Seismic Sequence in the Santorini-Amorgos Region: Insights Into Volcano-Tectonic Activity Through High-Resolution Seismic Monitoring* © 2025 by Ioannis Fountoulakis is licensed under CC BY 4.0.